CLINICAL ORAL IMPLANTS RESEARCH

Simone F. M. Janner
Marco D. Caversaccio
Patrick Dubach
Pedram Sendi
Daniel Buser
Michael M. Bornstein

Characteristics and dimensions of the Schneiderian membrane: a radiographic analysis using cone beam computed tomography in patients referred for dental implant surgery in the posterior maxilla

Authors' affiliations:
Simone F. M. Janner, Daniel Buser, Michael M. Bornstein, Department of Oral Surgery and Stomatology, School of Dental Medicine, University of Bern, Bern, Switzerland
Marco D. Caversaccio, Patrick Dubach, Clinic for Ear, Nose and Throat Diseases, Head and Neck Surgery, Bern University Hospital, University of Bern, Bern, Switzerland
Pedram Sendi, Institute for Clinical Epidemiology & Biostatistics, Basel University Hospital, Basel, Switzerland

Corresponding author:
PD Dr Michael M. Bornstein
Department of Oral Surgery and Stomatology
School of Dental Medicine
University of Bern
Freiburgstrasse 7
3010 Bern
Switzerland
Tel.: +41 31 632 25 45/66
Fax: +41 31 632 09 14
e-mail: michael.bornstein@zmk.unibe.ch

Date:
Accepted 7 December 2010

To cite this article:
Janner SFM, Caversaccio MD, Dubach P, Sendi P, Buser D, Bornstein MM. Characteristics and dimensions of the Schneiderian membrane: a radiographic analysis using cone beam computed tomography in patients referred for dental implant surgery in the posterior maxilla.
Clin. Oral Impl. Res. **xx**, 2011; 000–000.
doi: 10.1111/j.1600-0501.2010.02140.x

Key words: cone beam computed tomography, dental implants, mucosal thickness, posterior maxilla, Schneiderian membrane, sinus floor elevation, volume tomography

Abstract

Objectives: To determine the dimensions of the Schneiderian membrane using limited cone beam computed tomography (CBCT) in individuals referred for dental implant surgery, and to determine factors influencing the mucosal thickness.

Material and methods: The study included 143 consecutive patients referred for dental implant placement in the posterior maxilla. A total of 168 CBCT images were taken using a limited field of view of 4 × 4 cm, 6 × 6 cm, or 8 × 8 cm. Reformatted coronal CBCT slices were analyzed with regard to the thickness and characteristics of the Schneiderian membrane in nine standardized points of reference. Factors such as age, gender, or status of the remaining dentition that could influence the dimensions of the Schneiderian membrane were evaluated using univariate and multivariate linear regression models.

Results: The thickness of the Schneiderian membrane exhibited a wide range, with a minimum value of 0.16 mm and a maximum value of 34.61 mm. The highest mean values, ranging from 2.16 to 3.11 mm, were found for the mucosa located in the mid-sagittal regions of the maxillary sinus. The most frequent mucosal findings diagnosed were flat thickenings of the Schneiderian membrane (62 positive findings, 37%). For the multivariate linear regression model, only gender had a statistically significant influence on the mean overall and mid-sagittal thickness of the sinus mucosa.

Conclusion: There is great interindividual variability in the thickness of the Schneiderian membrane. Gender seems to be the most important parameter influencing mucosal thickness in asymptomatic patients. Future studies are needed to assess the therapeutic and prognostic consequences of mucosal alterations in the maxillary sinus.

Since the first description in 1998 (Mozzo et al. 1998), cone beam computed tomography (CBCT) has become a popular and important technique for diagnosis and treatment planning in dental medicine (Ziegler et al. 2002; Bremke et al. 2008). It has already become an established diagnostic tool for some indications, such as endodontics (Lofthag-Hansen et al. 2007; Patel 2009), dental traumatology (Bornstein et al. 2009), apical surgery (Rigolone et al. 2003; Low et al. 2008; Bornstein et al. 2010), challenging periodontal bone defects (Misch et al. 2006; Kasaj & Willershausen 2007), preoperative planning of furcation surgery (Walter et al. 2009), and dental implant surgery (Guerrero et al. 2006). Even for visualization of the paranasal sinuses, for which conventional computed tomography (CT) is considered the diagnostic method of choice (Fatterpekar et al. 2008), CBCT imaging is becoming more popular (Ziegler et al. 2002; Bremke et al. 2008).

The placement of endosseous dental implants has become an established and very common surgical procedure in dentistry over the past three decades. In the posterior maxilla, reduced bone height and low bone density are the most common limitations for implant placement (Jemt & Lekholm 1995). Sinus floor elevation (SFE) procedures have been documented as predictable surgical options to overcome this obstacle (Bornstein et al. 2008). Radiographic findings that sometimes may pose problems for the surgeon planning an SFE procedure with or without simultaneous dental implant placement are the presence of bony septa (Naitoh et al. 2009), thickening of the Schneiderian membrane, prior

destructive maxillary sinus surgery (e.g., Caldwell-Luc operation), and manifest pathology such as acute rhinosinusitis or neoplastic processes (van den Bergh et al. 2000). There is only limited knowledge of the mean thickness and the dimension of the Schneiderian membrane, and there are no guidelines for assessment and classification of mucosal findings in the maxillary sinus before SFE.

The objective of the present study was to analyze the thickness and the anatomic characteristics of the Schneiderian membrane using limited CBCT in patients referred for dental implant placement in the posterior maxilla. Additionally, the influence of age, gender, smoking habits, periodontal and endodontic findings, and the time period elapsed since the last tooth removal in the region of interest on the dimensions and morphology of the maxillary sinus mucosa were evaluated.

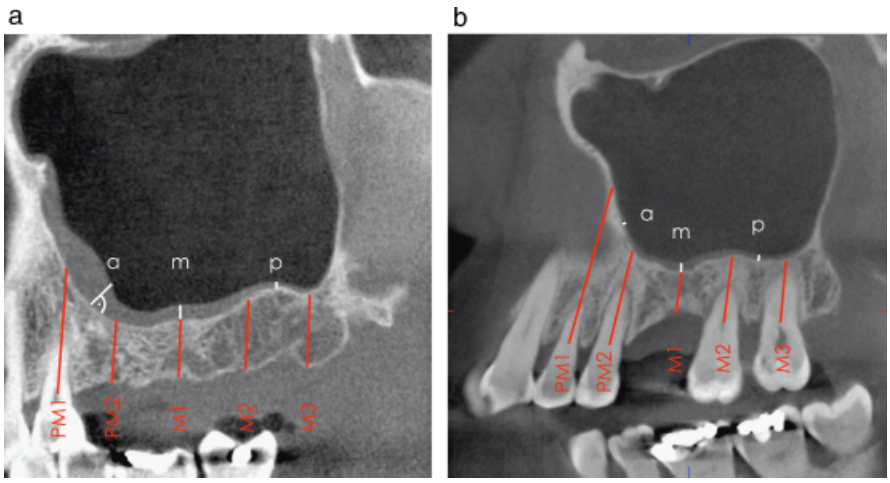

Fig. 1. Location of the measurement regions in the sagittal cone beam computed tomography slices: anterior region (a; PM1, first premolar; PM2, second premolar), middle region (m; M1, first molar), and posterior region (p; M2, second molar; M3, third molar). Patient with a distal extension situation in the left posterior maxilla (a); patient with a single tooth gap in the left posterior maxilla (b).

Material and methods

Patient selection

For the present study, all partially edentulous patients scheduled for limited CBCT imaging for further radiographic evaluation of a future implant insertion site in the posterior maxilla (first premolar to second molar) were consecutively enrolled. All patients had been referred by their private dentist to the Department of Oral Surgery and Stomatology at the University of Bern for implant therapy. The CBCT image taking occurred in the period between January 1, 2008 and December 31, 2008. Patients with a history of previous dental implant placement or bone grafting in the posterior maxilla, reduced sinus visibility in the CBCT scan volume (less than the region of the anterior maxillary sinus border to the second molar in the sagittal slices; floor of the nose and/or onset of the zygomatic process not visible in the coronal slices), or with evident artifacts due to movement during image taking were excluded from the present study.

At the time of the retrospective data analysis, the implant therapy planning, and in most cases, the implant surgery had already been performed.

Imaging procedure

The CBCT images were obtained with a 3D Accuitomo XYZ Slice View Tomograph (Morita, Kyoto, Japan) with a voxel size of 0.08 mm. Operating parameters were set at 5.0 to 7.0 mA and 80 kV and exposure time was 17.5 s. For all CBCT images, a limited field of view (FOV) of 4 × 4 cm, 6 × 6 cm, or 8 × 8 cm was selected. The data were reconstructed with slices at an interval of 0.5 mm.

Evaluation of the images

The CBCT images were evaluated by an experienced graduate student not directly involved in the treatment and follow-up of the patients (S. J.). For knowledge and diagnostic skills of maxillary sinus pathologies, the graduate student was instructed by two ENT specialists. For calibration and evaluation of intraexaminer reliability, 10 randomly selected cases were measured twice on two different days, resulting in a mean difference of 0.18 mm per image (range of 0–0.33 mm). For the further study, each measurement was repeated, and the mean value was calculated. When the difference between two values was ≥ 0.2 mm, a third measurement was performed (Bornstein et al. 2010). CBCT images were analyzed using a Dell 380 Precision workstation (Dell SA, Geneva, Switzerland) and a 19 in. Eizo Flexscan monitor with a resolution of 1280 × 1024 pixels (Eizo Nanao AG, Wädenswil, Switzerland). The analyses and measurements described below were performed using a specialized computer software (i-Dixel Version 1.8, Morita).

Measurements to determine the thickness of the Schneiderian membrane

The CBCT slices were first reformatted to place the posterior maxillary segment (first premolar to second molar) of the alveolar bone crest in a vertical position in the axial slices, and the palate/floor of the nose in a horizontal position in the coronal slices. Subsequently, three standardized measurements of the dimensions of the Schneiderian membrane in millimeters were performed using the coronal CBCT slice in the anterior region of the maxillary sinus in the lateral (alat), in the mid-sagittal (amid), and in the medial (amed) aspect. The selected anterior slice of the maxillary sinus floor corresponds to the region between the root tips of the maxillary premolars in a dentate patient (Fig. 1). The following anatomic landmarks in the coronal CBCT slices were selected for standardized measurements at each position (Fig. 2a–c):

(1) The onset of the zygomatic process for the lateral measurement (= alat).
(2) The deepest point of the sinus floor in the coronal CBCT slice for the mid-sagittal measurement (= amid).
(3) The ipsilateral bony floor of the nose for the medial measurement (= amed).

In cases where the sinus floor was located more cranial than the onset of the zygomatic process, or than the bony floor of the nose, the lateral (lat) – respectively, the medial (med) – measurements were performed at the height of the onset of the ipsilateral inferior nasal choncha. These three measurements were repeated in the middle region (Fig. 1, see marking m), corresponding to the apex of the first maxillary molar (mlat, mmid, mmed), and in the posterior region (Fig. 1, see marking p), corresponding to the region between the apex of the second and the third maxillary molars in dentate patients (plat, pmid, pmed). In edentulous posterior sites, distances between premolar roots were set at 7 mm, and distances between molar roots at 8 mm. Therefore, the radiographic evaluation included nine separate measurements for each maxillary sinus analyzed (Fig. 3). All measurements of the mucosal thickness were performed perpendicularly to the underlying bone, starting at the underlying bony plate and ending at the mucosal surface.

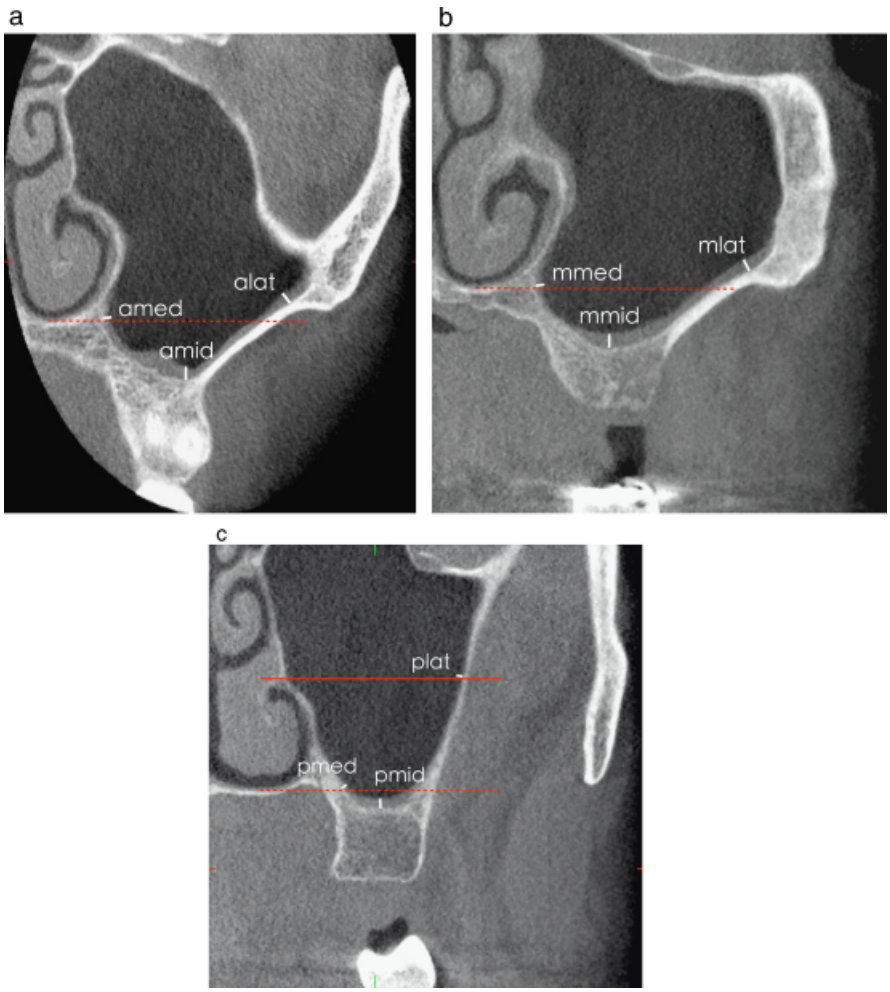

Fig. 2. Landmarks for the measurement of the mucosa thickness in coronal cone beam computed tomography slices in the anterior (a), middle (b), and posterior (c) regions: the onset of the zygomatic process for the lateral measurement (lat); the deepest point of the sinus floor for the mid-sagittal measurement (mid); the ipsilateral bony floor of the nose for the medial measurement (med). The red dotted line indicates the position of the bony floor of the nose; the continuous red line indicates the inferior nasal choncha.

Mucosal thickening of >2 mm was classified as pathological, and was classified according to criteria adapted from Soikkonen & Ainamo (1995):

(1) Flat: shallow thickening without well-defined outlines.
(2) Semi-aspherical: thickening with well-defined outlines rising in an angle of $>30^{\circ}$ from the floor or the walls of the sinus.
(3) Mucocele-like: complete opacification of the sinus.
(4) Mixed flat and semi-aspherical thickenings.
(5) Other mucosal thickening types or pathological findings.

The following findings of the teeth (canines, premolars, and molars including the third molar) in the region of interest were evaluated by screening the corresponding CBCT sections in all three dimensions (sagittal, coronal, and axial):

(1) Status of the dentition in the posterior maxilla: single tooth gap, multiple tooth gap, distal extension situation, edentulous.
(2) Presence of endodontically treated teeth (yes/no in anterior, middle, and posterior maxillary sinus regions).
(3) Presence of apical lesions according to the diagnostic criteria of Low et al. (2008) in the region of interest (yes/no in anterior, middle, and posterior maxillary sinus regions): a periapical radiolucency in connection with the apical part of the root was classified as a lesion when the width of the radiolucency exceeded at least twice the width of the periodontal ligament space, and the lesion was visible in at least two image planes.
(4) Presence of periodontal lesions (positive for radiographic marginal bone loss deeper than the midlevel of the respective root or involvement of furcation in molars) in the regions of interest (yes/no in anterior, middle, and posterior maxillary sinus regions).

Additional clinical and radiographic parameters assessed

The season in which the CBCT image was taken (winter, spring, summer, autumn) was recorded for further evaluation as a potential parameter influencing the thickness of the Schneiderian membrane.

The following anamnestic parameters of the included patients were recorded:

(1) Age and gender.
(2) Tobacco use, classified as current, former, or never smoker.
(3) Known rhinologic disease.
(4) Weeks since last tooth/teeth removal in the examined maxillary segment.

Statistical analysis

All data were first analyzed using descriptive statistics and box plots. In addition, the 95% confidence intervals of the mean thickness measures were calculated for the different patient subgroups. The impact of potential influencing parameters on the mean values for the overall thickness (nine measurements per maxillary sinus) and mid-sagittal thickness (three values per maxillary sinus) of the Schneiderian membrane was evaluated using univariate and multivariate linear regression models. Each sinus was considered as independent because asymmetrical thickness of the Schneiderian membrane was suspected in patients. The response variable (thickness of the Schneiderian membrane) was log-transformed for further analysis to achieve normality because the original data were skewed. All parameters with a P-value of 0.2 or less in the univariate analysis were included for further analysis in a multivariate linear regression model. The fit of the models was assessed by evaluating the residuals of the respective regression models. In addition, a robust regression was performed on the log-transformed response variable to assess whether the coefficients and standard errors would vary when more robust methods are used (Draper & Smith 1998). The significance level chosen for all statistical tests was $P \leq 0.05$. All analyses were performed using a software package (Stata 11, Stata Corp., College Station, TX, USA).

Results

During the study period, a total of 199 patients were included for potential analysis of their CBCT images with respect to the dimensions and anatomic characteristics of the basal Schneiderian membrane. In two limited CBCTs, the

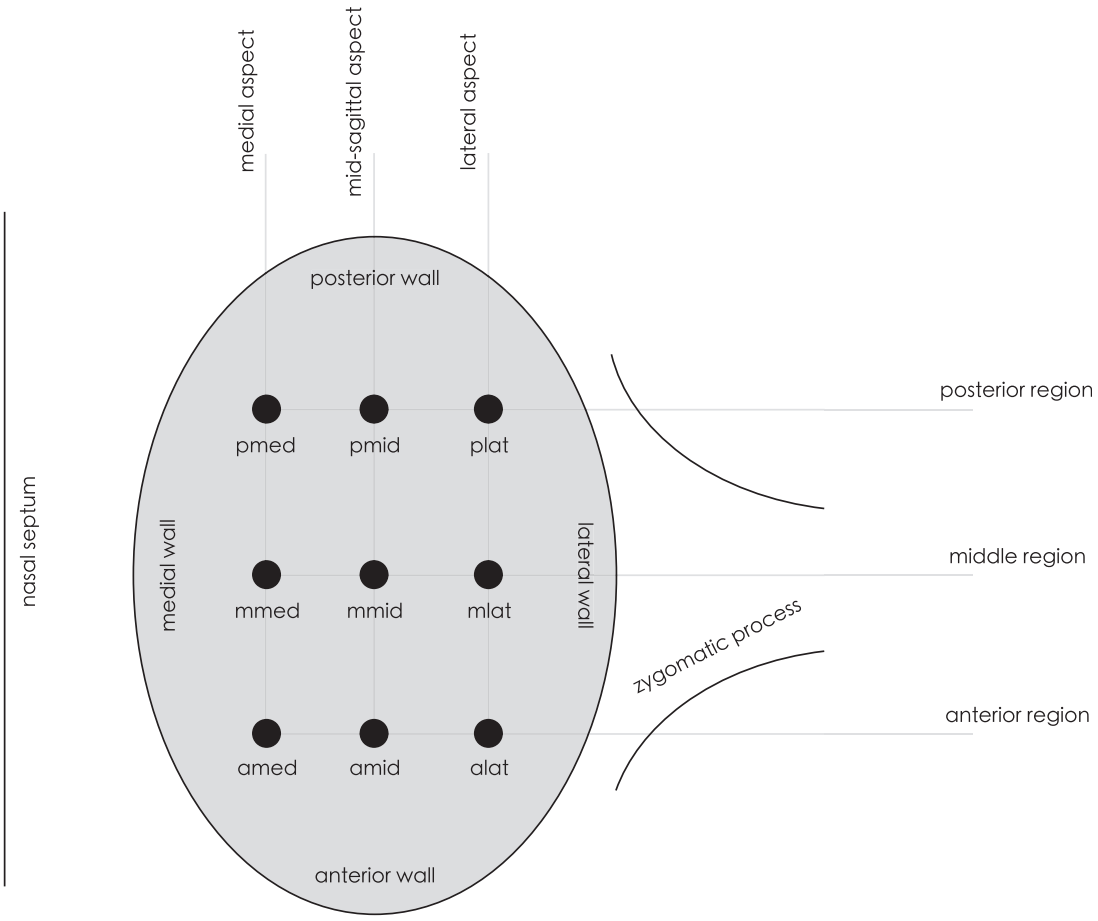

Fig. 3. Schematic overview of the nine measurement points in the evaluated maxillary sinuses (axial slice).

Table 1. **Analysis of the thickness (in mm) of the Schneiderian membrane using coronal slices from limited CBCT images**

Measurement	Anterior			Middle			Posterior		
	alat	amid	amed	mlat	mmid	mmed	plat	pmid	pmed
Mean	0.96	2.47	1.6	1.11	3.11	1.84	0.9	2.16	0.99
Median	0.63	1.13	0.66	0.56	1.41	0.66	0.52	0.88	0.56
Maximum	21.08	30	16.5	26.67	34.61	22.33	21.41	30.51	15.27
Minimum	0.16	0.28	0.18	0.18	0.25	0.25	0.25	0.25	0.16
95% CI	0.69–1.22	1.89–3.04	1.2–2.01	0.75–1.47	2.4–3.82	1.3–2.39	0.58–1.22	1.57–2.76	0.7–1.28

Measurements for "anterior," "middle," and "posterior" correspond to the regions shown in Figs 2a–c and 3.
CBCT, cone beam computed tomography; CI, confidence interval.

analysis of the images was not possible due to movement artifacts; 20 patients had a history of dental implant placement or bone grafting in the posterior maxilla; and in 34 patients the visible area of the maxillary sinus in the FOV did not meet the inclusion criteria mentioned above. This resulted in a total of 143 patients with 168 CBCT scans included in the present study. This group comprised 67 men and 76 women with a mean age of 57.5 years (± 11.67). Of the included patients, 21 were current smokers, 15 were former smokers, and 96 reported never having used tobacco. In 11 patients, the status of tobacco use was not reported. The patients included in the study exhibited 64 single tooth gaps, 37 multiple tooth gaps, and 50 distal extension situations, and 17 patients were edentulous.

Descriptive analysis of the dimensions and characteristics of the Schneiderian membrane

There was a wide range in the thickness of the Schneiderian membrane as evaluated on the CBCT images, with a minimum value of 0.16 mm and a maximum value of 34.61 mm (Table 1). The highest mean values, ranging from 2.16 to 3.11 mm, were found for the mucosa located in the mid-sagittal regions of the maxillary sinus, whereas the mean values of the mucosal dimensions on the lateral and medial aspects of the maxillary sinus varied between 0.9 and 1.84 mm. The median values were lower for all regions analyzed, and more pronounced for the three mid-sagittal measurements. For all three regions analyzed (anterior, middle, and posterior), the mid-sagittal values were statistically significantly different from the respective measurements in the lateral and medial walls of the maxillary sinus.

In the descriptive analysis of the CBCT images, 76 maxillary sinuses (45% out of a total of 168) were classified as healthy (Table 2). The most frequent pathologies diagnosed were flat

Table 2. **Types of pathology and thickness (in mm) of the Schneiderian membrane according to the season of image taking as diagnosed on CBCT images**

Season	Number of CBCTs, *n*	Pathology in maxillary sinus (yes/no), *n* (%)	Type of pathology (0–5) *n* (%)			Mean thickness lat in mm (95% CI)	Mean thickness mid in mm (95% CI)	Mean thickness med in mm (95% CI)	Mean overall thickness in mm (95% CI)
Spring	36	16 (44.44)	0	20	55%	1.8 (0.48–3.11)	4.11 (1.9–6.31)	2.36 (1–3.71)	2.75 (1.19–4.32)
			1	7	20%				
			2	5	14%				
			3	–	–				
			4	4	11%				
			5	–	–				
Summer	39	18 (46.15)	0	21	54%	0.7 (0.54–0.86)	1.91 (1.29–2.54)	1.21 (0.8–1.62)	1.28 (0.92–1.63)
			1	14	36%				
			2	2	5%				
			3	–	–				
			4	–	–				
			5	2	5%				
Autumn	57	36 (63.16)	0	21	37%	0.83 (0.58–1.08)	2.05 (1.49–2.61)	1.15 (0.78–1.52)	1.34 (0.97–1.72)
			1	27	47%				
			2	1	2%				
			3	–	–				
			4	4	7%				
			5	4	7%				
Winter	36	22 (61.11)	0	14	39%	0.75 (0.57–0.92)	2.62 (1.38–3.86)	1.41 (0.46–2.36)	1.59 (0.85–2.33)
			1	14	39%				
			2	4	11%				
			3	1	3%				
			4	3	8%				
			5	–	–				
Total	168	92 (54.76)	0	76	45%	0.99 (0.69–1.28)	2.58 (1.99–3.16)	1.48 (1.09–1.86)	1.68 (1.28–2.08)
			1	62	37%				
			2	12	7%				
			3	1	1%				
			4	11	6%				
			5	6	4%				

CBCT, cone beam computed tomography; CI, confidence interval.

Table 3. **Tooth-related potential influencing factors in the analyzed region and thickness (in mm) of the Schneiderian membrane as diagnosed on CBCT images**

Region	Endodontically treated teeth in ROI% (95% CI)	Apical lesions in ROI% (95% CI)	Periodontal lesions in ROI% (95% CI)	Mean midline-value in mm (95% CI)
Anterior	19.64 (13.57–25.71)	19.05 (13.05–25.05)	4.76 (1.51–8.02)	2.46 (1.89–3.04)
Middle	13.69 (8.43–18.94)	13.69 (8.44–18.94)	7.74 (3.66–11.82)	3.11 (2.4–3.82)
Posterior	10.71 (5.98–15.44)	9.52 (5.04–14.01)	8.33 (4.11–12.56)	2.16 (1.57–2.76)
Total	14.68 (11.27–18.09)	14.09 (10.6–17.58)	6.94 (4.47–9.42)	2.58 (2–3.17)

ROI, region of interest; midline-value, thickness of the Schneiderian membrane as measured in the deepest aspect of the maxillary sinus floor; CBCT, cone beam computed tomography; CI, confidence interval.

thickenings of the Schneiderian membrane (62 positive findings in 168 maxillary sinuses/37%). Only one case of a mucocele-like radioopacity in the respective sinus was found.

Analysis of potential factors influencing the dimensions and characteristics of the Schneiderian membrane

The presence of endodontically treated teeth in the region of interest decreased from 19.64% in the anterior region to 13.69% in the middle region to 10.71% in the posterior region of the maxillary sinuses analyzed (Table 3). A similar distribution was observed for apical lesions: 19.05% were diagnosed in the anterior, 13.69% in the middle, and 9.52% in the posterior region. Periodontal lesions exhibited an inverse distribution pattern, with 4.76% of the pathologies diagnosed in anterior regions, 7.74% in middle regions, and 8.33% in posterior regions of the maxillary sinuses. The mean time elapsed since the last tooth removal in the analyzed segment as reported by the patient was 146.26 weeks (SD ± 247.9).

For the univariate linear regression model, gender ($P = 0.004$) of the patients and periapical status of the teeth in the region of interest ($P = 0.0033$) exhibited a statistically significant influence on the mean overall and mid-sagittal thickness of the Schneiderian membrane (Table 4). The respective mean values were generally higher for male subjects and for teeth with evident periapical pathology. No statistically significant influence was seen for age ($P = 0.174$), rhinologic disease ($P = 0.727$), tobacco use ($P = 0.411$), last tooth removal in the examined maxillary segment ($P = 0.179$), endodontic ($P = 0.312$) and periodontal status ($P = 0.106$) of the dentition in the region of interest, and the season of CBCT image taking (P-values from 0.335 to 0.663; Table 4). For the multivariate linear regression model, only gender had a statistically significant influence on the mean overall and mid-sagittal thickness of the Schneiderian membrane ($P = 0.01$ for overall mean thickness; $P = 0.015$ for mean mid-sagittal thickness; Table 5).

Discussion

More than 90% of the epithelial cells of the Schneiderian membrane are ciliated and distributed in a single, columnar, pseudostratified layer. The beat frequency of the cilia is approximately 60 kHz, thus moving mucus and debris actively

Table 4. **Univariate analysis of potential influencing clinical and anamnestic parameters of the mean overall and mean mid-sagittal thickness (in mm) of the Schneiderian membrane**

Factor	Overall mean thickness			Mean mid-sagittal thickness		
	Coefficient	*T*-value	*P*-value	Coefficient	*T*-value	*P*-value
Age	0.06	1.37	0.174	0.07	1.3	0.194
Gender (female vs. male)	**−0.33**	**−2.92**	**0.004**	**−0.37**	**−2.76**	**0.007**
Rhinologic disease	0.08	0.35	0.727	0.14	0.51	0.631
Tobacco use	−0.13	−0.83	0.411	−0.15	−0.84	0.402
Time since extraction	0.02	1.35	0.179	0.02	0.85	0.395
Endodontic status	0.12	1.02	0.312	0.148	1.03	0.305
Periapical status	**0.26**	**2.15**	**0.033**	**0.305**	**2.1**	**0.037**
Periodontal status	0.24	1.62	0.106	0.308	1.72	0.087
Season of imaging*						
2 vs. 1	0.17	0.97	0.335	0.11	0.54	0.588
3 vs. 1	−0.12	−0.67	0.506	−0.18	−0.88	0.382
4 vs. 1	−0.07	−0.44	0.663	−0.09	−0.51	0.61

The response variable (thickness of the Schneiderian membrane) was log-transformed for further analysis. Bold indicates statistically significant results.
*Partial *F* test for all four seasons (1, winter; 2, spring; 3, summer; 4, autumn; overall mean thickness $P = 0.3612$, mean mid-thickness $P = 0.5087$).

Table 5. **Multivariate analysis of potential influencing anamnestic and clinical parameters on the mean overall and mean mid-sagittal thickness (in mm) of the Schneiderian membrane**

Factor	Overall mean thickness			Mean mid-sagittal thickness		
	Coefficient	*T*-value	*P*-value	Coefficient	*T*-value	*P*-value
Age	0.04	0.82	0.412	0.04	0.75	0.454
Gender (female vs. male)	**−0.31**	**−2.61**	**0.01**	**−0.33**	**−2.46**	**0.015**
Periapical status	0.2	1.54	0.124	0.23	1.49	0.139
Periodontal status	0.1	0.64	0.525	0.15	0.78	0.435

The response variable (thickness of the Schneiderian membrane) was log-transformed for further analysis. Bold indicates statistically significant results.

toward the natural ostium (van den Bergh et al. 2000; Pikos 2008). Factors compromising mucous production and clearance of the mucosa can increase the risk of sinusitis development and have to be avoided. A typical example of such a risk factor in dentistry is the penetration of particulate graft material during sinus floor surgery (Pikos 2008). The mean thickness of the Schneiderian membrane was evaluated in a post-mortem study with values ranging from 0.3 to 0.8 mm in 10 unfixed, fresh cadavers without signs of sinusitis (Tos & Mogensen 1979). In a similar study using 20 fresh cadavers, Pommer et al. (2009) found a mean thickness value of 0.09 ± 0.05 mm (range 0.02–0.35 mm). In a study analyzing sinus biopsies from healthy subjects, Aimetti et al. (2008) measured a mean thickness of 0.97 ± 0.36 mm. All three groups describe great interindividual variability in the thickness of the Schneiderian membrane.

Existing data on the dimensions and changes in the Schneiderian membrane based on radiographic imaging are rare in the literature. In CT and magnetic resonance imaging (MRI) studies, coronal slices are well established for evaluating the mucosal thickness in the maxillary sinus, and the measurements are always performed perpendicular to the underlying bone (Rak et al. 1991; Min et al. 1994; Peleg et al. 1999; Pruna 2003; Cagici et al. 2009). Nevertheless, the location of the measurement points utilized in these studies varies greatly. Additionally, studies apply different measurement scales and classifications from the maximum mucosal thickness in millimeters (Rak et al. 1991), to the simple description of the shape of mucosal thickening (Soikkonen & Ainamo 1995; Patel et al. 1996), and finally to the detection of changes in membrane thickness over time (Min et al. 1994; Peleg et al. 1999). Furthermore, early reports of thickness measurements revealed difficulty in visualizing normal mucoperiosteal structures in the paranasal sinuses through CT (Min et al. 1994) or MRI (Patel et al. 1996). The mucosa could be seen only at a thickness of 2 mm or above, and therefore historically 2 mm was considered a reliable threshold for pathological mucosal swelling (Cagici et al. 2009).

The results of the present study confirmed the great interindividual variability of the thickness of the Schneiderian membrane, with values ranging from 0.16 mm (minimum) to 34.61 mm (maximum). Furthermore, a discrepancy between mean and median values was evident, suggesting that some of the subjects analyzed exhibited very high mucosal thickness values (Table 1). When only interpreting the mean mucosal thickness values, the mid-sagittal findings in anterior, middle, and posterior regions have to be considered as pathological according to Cagici et al. (2009). However, the median values for all nine regions evaluated ranged from 0.52 to 1.41 mm.

When comparing mean and median values, the Schneiderian membrane was the thinnest in the lateral measurements, with slightly higher values in the median aspect, and statistically significantly higher values in the mid-sagittal aspect. It can be speculated that the mid-sagittal thickness values are increased because of the seated patient position during CBCT image taking, which could cause the accumulation of mucous secretions in the deepest aspect of the maxillary sinus. Other imaging techniques, such as MRI, CT, and sometimes CBCT, perform image taking on a prone patient. Moreover, CBCT imaging does not allow differentiation between liquids and soft tissue. Therefore, the high mean/median values for the mid-sagittal measurements could also be partially due to mucous accumulation on the Schneiderian membrane.

A high prevalence of mucosal thickening in paranasal sinuses of asymptomatic patients is reported in the literature. The analysis of 9315 panoramic radiographs in a Finnish health survey revealed maxillary mucosal thickening in 12% of the subjects, and a prevalence of mucous antral cysts of 7% (Vallo et al. 2010). Incidental paranasal mucosal changes were also evaluated in MRI scans performed for diagnosis of neurological pathologies (Cooke & Hadley 1991; Patel et al. 1996). The highest prevalence was reported for the ethmoidal sinuses, followed by the maxillary sinuses. The maxillary sinuses had a prevalence of shallow/flat mucosal thickening ranging from 23% to 31%, and a prevalence of cystic lesions ranging from 7% to 10%. In these studies, the authors did not use any threshold values for classification of pathologies, but only a description of the shape. A prospective radiographic analysis of 666 patients undergoing CT scans for indications such as head injuries or seizures reported abnormalities of one or more of the paranasal sinuses in 42.5% of the patients (Havas et al. 1988). In the present analysis, a higher prevalence of mucosal pathologies (55%) was found than in the studies mentioned above. This could be due to the use of a precise threshold value to define a pathologic Schneiderian membrane (2 mm). Nevertheless, the clinical significance of this value has to be regarded with some caution, as it remains to be addressed in future studies, how many of these findings and which type of mucosal thickening require therapy. The prevalence of cystic-shaped lesions was 7%, demonstrating good correlation with previous studies (Cooke & Hadley 1991; Patel et al. 1996; Vallo et al. 2010).

The available literature describing potential local or systemic influences on the thickness of

the Schneiderian membrane identifies many different factors. In a study using intraoral radiographs, Engström et al. (1988) found a mean sinus floor mucosal thickness of 5.6 ± 6.1 mm before and 0.6 ± 1.6 mm after extensive periodontal therapy in the corresponding sextant for 13 patients with advanced periodontal disease. Gingival thickness and gender were the only genetically determined parameters to reliably predict sinus membrane thickness, being higher in patients with thick gingival biotype and lower in women (Aimetti et al. 2008; Vallo et al. 2010). An analysis of 330 maxillary sinuses on CT scans revealed a statistically significantly higher prevalence of mucosal thickening in proximity to restored teeth (Connor et al. 2000). Vallo et al. (2010) found higher Schneiderian membrane thickness values in maxillary sinuses adjacent to periodontal and endodontic lesions. Furthermore, smoking and the presence of rhinologic diseases correlated with increased mucosal thickness. The month in which images were taken was reported to have an influence on pathologic findings in the maxillary sinuses, with September, October, and November having a higher prevalence of cystic lesions (Rodrigues et al. 2009; Vallo et al. 2010), and an increased prevalence of mucosal thickening during winter (Tarp et al. 2000).

In the present study, only gender was identified as an influencing factor for maxillary sinus mucosa thickness in the multivariate regression analysis, with male subjects having higher mean values. Endodontic, periodontal, and periapical status of the dentition in the region of interest had no statistically significant influence. This could be due to the difference in the populations analyzed. To further evaluate the potential impact of dental pathologies of teeth in the posterior maxilla on the dimensions of the Schneiderian membrane, prospective cohort studies with larger samples and specific problems (periodontal, periapical/endodontic) are needed.

The most frequent surgical complication reported to occur during SFE is an accidental perforation of the Schneiderian membrane, occurring in 10–56% of the operated sinuses (Bornstein et al. 2008; Pikos 2008). Other postoperative complications include acute or chronic sinus infection, bleeding, wound dehiscence, exposure of the barrier membrane, and graft loss (Regev et al. 1995; Pikos 2006). To the best of our knowledge, the impact of the condition of the Schneiderian membrane on the success and long-term outcome of dental implant placement has not yet been evaluated in the literature. Nevertheless, a recent case series analyzing failures of SFE procedures reported that out of 13 patients included, preoperative chronic maxillary sinusitis had been present in four patients (Anavi et al. 2008). The authors therefore stated that elimination of sinusitis and other potential pathological conditions is necessary before SFE. What therapeutic significance has to be attributed to the relative high prevalence of mucosal findings (55%), and which of these need further evaluation and eventual treatment, has not been analyzed in the present study. As there are no guidelines for classification and treatment of mucosal findings in the maxillary sinus before SFE, future prospective studies are needed. These studies should also analyze patency of the osteomeatal complex and the condition of the bony walls of the maxillary sinuses.

Because of the complex anatomical situation in the posterior maxilla, cross-sectional imaging (CT scan) has been proposed as the standard radiographic method for preoperative planning of dental implant placement (Dula et al. 2001; Harris et al. 2002). In the present study, limited CBCT was used to visualize the posterior maxilla, including the soft tissue morphology of the related maxillary sinus. Smaller FOV should always be used when possible, thus adhering to the ALARA (as low as reasonably achievable) principle in medical radiology (McCollough et al. 2009). In comparison with CT, modern CBCT devices have the advantage of administering less radiation to the patient (Cohenca et al. 2007; Suomalainen et al. 2009; Okano et al. 2009). Therefore, CBCT can be regarded as an alternative to CT for three-dimensional imaging before SFE.

References

Aimetti, M., Massei, G., Morra, M., Cardesi, E. & Romano, F. (2008) Correlation between gingival phenotype and Schneiderian membrane thickness. *The International Journal of Oral & Maxillofacial Implants* **23**: 1128–1132.

Anavi, Y., Allon, D.M., Avishai, G. & Calderon, S. (2008) Complications of maxillary sinus augmentations in a selective series of patients. *Oral Surgery, Oral Medicine, Oral Pathology, Oral Radiology, and Endodontics* **106**: 34–38.

Bornstein, M.M., Chappuis, V., von Arx, T. & Buser, D. (2008) Performance of dental implants after staged sinus floor elevation procedures: 5-year results of a prospective study in partially edentulous patients. *Clinical Oral Implants Research* **19**: 1034–1043.

Bornstein, M.M., Lauber, R., Sendi., P. & von Arx, T. (2010) Comparison of periapical radiography and limited cone beam computed tomography in mandibular molars for analysis of anatomical landmarks prior to apical surgery. *Journal of Endodontics* (accepted for publication).

Bornstein, M.M., Wölner-Hanssen, A.B., Sendi, P. & von Arx, T. (2009) Comparison of intraoral radiography and limited cone beam computed tomography for the assessment of root-fractured permanent teeth. *Dental Traumatology* **25**: 571–577.

Bremke, M., Sesterhenn, A.M., Murthum, T., Hail, A.A., Kadah, B.A., Bien, S. & Werner, J.A. (2008) Digital volume tomography (DVT) as a diagnostic modality of the anterior skull base. *Acta Oto-Laryngologica* **31**: 1–9.

Cagici, C.A., Yilmazer, C., Hurcan, C., Ozer, C. & Ozer, F. (2009) Appropriate interslice gap for screening coronal paranasal sinus tomography for mucosal thickening. *European Archives of Oto-Rhino-Laryngology* **266**: 519–525.

Cohenca, N., Simon, J.H., Roges, R., Morag, Y. & Malfaz, J.M. (2007) Clinical indications for digital imaging in dento-alveolar trauma. Part 1: traumatic injuries. *Dental Traumatology* **23**: 95–104.

Connor, S.E., Chavda, S.V. & Pahor, A.L. (2000) Computed tomography evidence of dental restoration as aetiological factor for maxillary sinusitis. *The Journal of Laryngology and Otology* **114**: 510–513.

Cooke, L. & Hadley, D. (1991) MRI of the paranasal sinuses: incidental abnormalities and their relationship to symptoms. *The Journal of Laryngology and Otology* **105**: 278–281.

Draper, N.R. & Smith, H. (1998) *Applied Regression Analysis*. 3rd edition. New York: Wiley-Interscience. 567–584.

Dula, K., Mini, R., van der Stelt, P.F. & Buser, D. (2001) The radiographic assessment of implant patients: decision-making criteria. *The International Journal of Oral & Maxillofacial Implants* **16**: 80–89.

Engström, H., Chamberlain, D., Kiger, R. & Egelberg J. (1988) Radiographic evaluation of the effect of initial periodontal therapy on thickness of the maxillary sinus mucosa. *Journal of Periodontology* **59**: 604–608.

Fatterpekar, G.M., Delman, B.N. & Som, P.M. (2008) Imaging the paranasal sinuses: where we are and where we are going. *The Anatomical Record* **291**: 1564–1572.

Guerrero, M.E., Jacobs, R., Loubele, M., Schutyser, F., Suetens, P. & van Steenberghe, D. (2006) State-of-the-art on cone beam CT imaging for preoperative planning of implant placement. *Clinical Oral Investigations* **10**: 1–7.

Harris, D., Buser, D., Dula, K., Grondahl, K., Haris, D., Jacobs, R., Lekholm, U., Nakielny, R., van Steenberghe, D. & van der Stelt, P. (2002) European Association for Osseointegration. E.A.O. guidelines for the use of diagnostic imaging in implant dentistry. A consensus workshop organized by the European Association for Osseointegration in Trinity College Dublin. *Clinical Oral Implants Research* **13**: 566–570.

Havas, T.E., Motbey, J.A. & Gullane, P.J. (1988) Prevalence of incidental abnormalities on computed tomographic scans of the paranasal sinuses. *Archives of Otolaryngology – Head & Neck Surgery* **114**: 856–859.

Jemt, T. & Lekholm, U. (1995) Implant treatment in edentulous maxillae: a 5-year follow-up report on patients with different degrees of jaw resorption. *The International Journal of Oral & Maxillofacial Implants* **10**: 303–311.

Kasaj, A. & Willershausen, B. (2007) Digital volume tomography for diagnostics in periodontology. *The International Journal of Computerized Dentistry* **10**: 155–168.

Lofthag-Hansen, S., Huumonen, S., Gröndahl, K. & Gröndahl, H.G. (2007) Limited cone-beam CT and intraoral radiography for the diagnosis of periapical pathology. *Oral Surgery, Oral Medicine, Oral Pathology, Oral Radiology, and Endodontics* **103**: 114–119.

Low, K.M., Dula, K., Bürgin, W. & von Arx, T. (2008) Comparison of periapical radiography and limited cone-beam tomography in posterior maxillary teeth referred for apical surgery. *Journal of Endodontics* **34**: 557–562.

McCollough, C.H., Primak, A.N., Braun, N., Kofler, J., Yu, L. & Christner, J. (2009) Strategies for reducing radiation dose in CT. *Radiologic Clinics of North America* **47**: 27–40.

Min, Y., Lee, J. & Shin, J. (1994) Radiologic assessment of diseased mucosa of the maxillary sinus after functional endoscopic sinus surgery. *Acta Otolaryngologica (Stockholm)* **114**: 657–662.

Misch, K.A., Yi, E.S. & Sarment, D.P. (2006) Accuracy of cone beam computed tomography for periodontal defect measurements. *Journal of Periodontology* **77**: 1261–1266.

Mozzo, P., Procacci, C., Tacconi, A., Martini, P.T. & Andreis, I.A. (1998) A new volumetric CT machine for dental imaging based on the cone-beam technique: preliminary results. *European Radiology* **8**: 1558–1564.

Naitoh, M., Suenaga, Y., Kondo, S., Gotoh, K. & Ariji, E. (2009) Assessment of maxillary sinus septa using cone-beam computed tomography: etiological consideration. *Clinical Implant Dentistry & Related Research* **11** (Suppl. 1): e52–e58.

Okano, T., Harata, Y., Sugihara, Y., Sakaino, R., Tsuchida, R., Iwai, K., Seki, K. & Araki, K. (2009) Absorbed and effective doses from cone beam volumetric imaging for implant planning. *Dentomaxillofacial Radiology* **38**: 79–85.

Patel, K., Chavda, S.V., Violaris, N. & Pahor, A.L. (1996) Incidental paranasal sinus inflammatory changes in a British population. *The Journal of Laryngology and Otology* **110**: 649–651.

Patel, S. (2009) New dimensions in endodontic imaging: Part 2. Cone beam computed tomography. *The International Endodontic Journal* **42**: 463–475.

Peleg, M., Chaushu, G., Mazor, Z., Ardekian, L. & Bakoon, M. (1999) Radiological findings of the post-sinus lift maxillary sinus: a computerized tomography follow-up. *Journal of Periodontology* **70**: 1564–1573.

Pikos, M.A. (2006) Complications of maxillary sinus augmentation. In: Jensen, O.T., ed. *The Sinus Bone Graft*. 2nd edition, 103–113. Chicago: Quintessence Publishing.

Pikos, M.A. (2008) Maxillary sinus membrane repair: update on technique for large and complete perforations. *Implant Dentistry* **17**: 24–31.

Pommer, B., Unger, E., Sütö, D., Hack, N. & Watzek, G. (2009) Mechanical properties of the Schneiderian membrane in vitro. *Clinical Oral Implants Research* **20**: 633–637.

Pruna, X. (2003) Morpho-functional evaluation of osteomeatal complex in chronic sinusitis by coronal CT. *European Radiology* **13**: 1461–1468.

Rak, K.M., Newell, J.D. II, Yakes, W.F., Damiano, M.A. & Luethke, J.M. (1991) Paranasal sinuses on MR images of the brain: significance of mucosal thickening. *American Journal of Roentgenology* **156**: 381–384.

Regev, E., Smith, R.A., Perrot, D.H. & Porgel, M.A. (1995) Maxillary sinus complications related to endosseous implants. *The International Journal of Oral & Maxillofacial Implants* **10**: 451–461.

Rigolone, M., Pasqualini, D., Bianchi, L., Berutti, E. & Bianchi, S.D. (2003) Vestibular surgical access to the palatine root of the superior first molar: ''low-dose cone-beam'' CT analysis of the pathway and its anatomic variations. *Journal of Endodontics* **29**: 773–775.

Rodrigues, C.D., Freire, G.F., Fonseca da Silveira, M.M. & Estrela, C. (2009) Prevalence and risk factors of mucous retention cysts in a Brazilian population. *Dentomaxillofacial Radiology* **38**: 480–483.

Soikkonen, K. & Ainamo, A. (1995) Radiographic maxillary sinus findings in the elderly. *Oral Surgery, Oral Medicine, Oral Pathology, Oral Radiology, and Endodontics* **80**: 487–491.

Suomalainen, A., Kiljunen, T., Käser, Y., Peltola, J. & Kortesniemi, M. (2009) Dosimetry and image quality of four dental cone beam computed tomography scanners compared with multislice computed tomography scanners. *Dentomaxillofacial Radiology* **38**: 367–378.

Tarp, B., Fiirgaard, B., Christensen, T., Jensen, J.J. & Black, F.T. (2000) The prevalence and significance of paranasal sinus abnormalities on MRI. *Rhinology* **38**: 33–38.

Tos, M. & Mogensen, C. (1979) Mucus production in the nasal sinuses. *Acta Oto-Laryngologica* **360**: 131–134.

Vallo, J., Suominen-taipale, L., Huumonen, S., Soikkonen, K. & Norblad, A. (2010) Prevalence of mucosal abnormalities of the maxillary sinus and their relationship to dental disease in panoramic radiography: results from the Health 2000 Health Examination Survey. *Oral Surgery, Oral Medicine, Oral Pathology, Oral Radiology, and Endodontics* **109**: e80–e87.

van den Bergh, J.P., ten Bruggenkate, C.M., Disch, F.J. & Tuinzing, D.B. (2000) Anatomical aspects of sinus floor elevations. *Clinical Oral Implants Research* **11**: 256–265.

Walter, C., Kaner, D., Berndt, D.C., Weiger, R. & Zitzmann, N.U. (2009) Three-dimensional imaging as a pre-operative tool in decision making for furcation surgery. *Journal of Clinical Periodontology* **36**: 250–257.

Ziegler, C.M., Woertche, R., Brief, J. & Hassfeld, S. (2002) Clinical indications for digital volume tomography in oral and maxillofacial surgery. *Dentomaxillofacial Radiology* **31**: 126–130.